ENVIRONMENTAL RESEARCH
LETTERS

LETTER • OPEN ACCESS

Unprecedented acceleration of winter discharge of Upper Yenisei River inferred from tree rings

ENVIRONMENTAL RESEARCH
LETTERS

OPEN ACCESS

RECEIVED
20 August 2021

REVISED
25 October 2021

ACCEPTED FOR PUBLICATION
29 November 2021

PUBLISHED
30 December 2021

LETTER

Unprecedented acceleration of winter discharge of Upper Yenisei River inferred from tree rings

Irina P Panyushkina[1,*], David M Meko[1], Alexander Shiklomanov[2], Richard D Thaxton[1], Vladimir Myglan[3], Valentin V Barinov[3] and Anna V Taynik[3]

[1] Laboratory of Tree-Ring Research, University of Arizona, 1215 E Lowell St.Tucson, AZ, 85721, United States of America
[2] Earth Systems Research Center, University of New Hampshire, Durham, NH, United States of America
[3] Siberian Federal University, Krasnoyarsk, Russia
[*] Author to whom any correspondence should be addressed.

E-mail: ipanyush@arizona.edu

Keywords: discharge tree-ring reconstruction, Siberian rivers, water balance model, Arctic amplification

Supplementary material for this article is available online

Abstract

The Yenisei River is the largest contributor of freshwater and energy fluxes among all rivers draining to the Arctic Ocean. Modeling long-term variability of Eurasian runoff to the Arctic Ocean is complicated by the considerable variability of river discharge in time and space, and the monitoring constraints imposed by a sparse gauged-flow network and paucity of satellite data. We quantify tree growth response to river discharge at the upper reaches of the Yenisei River in Tuva, South Siberia. Two regression models built from eight tree-ring width chronologies of *Larix sibirica* are applied to reconstruct winter (Nov–Apr) discharge for the period 1784–1997 (214 years), and annual (Oct–Sept) discharge for the period 1701–2000 (300 years). The Nov–Apr model explains 52% of the discharge variance whereas Oct–Sept explains 26% for the calibration intervals 1927–1997 and 1927–2000, respectively. This new hydrological archive doubles the length of the instrumental discharge record at the Kyzyl gauge and resets the temporal background of discharge variability back to 1784. The reconstruction finds a remarkable 80% upsurge in winter flow over the last 25 years, which is unprecedented in the last 214 years. In contrast, annual discharge fluctuated normally for this system, with only a 7% increase over the last 25 years. Water balance modeling with CRU data manifests a significant discrepancy between decadal variability of the gauged flow and climate data after 1960. We discuss the impact on the baseflow rate change of both the accelerating permafrost warming in the discontinuous zone of South Siberia and widespread forest fires. The winter discharge accounts for only one third of the annual flow, yet the persistent 25 year upsurge is alarming. This trend is likely caused by Arctic Amplification, which can be further magnified by increased winter flow delivering significantly more fresh water to the Kara Sea during the cold season.

1. Introduction

The inflow of freshwater and heat to the Arctic Ocean from rivers is of central importance to global climate variability via impacts on Arctic sea-ice coverage and the ocean's thermohaline circulation (Aagaard and Carmack 1989, Rahmstorf 2002, Fichot *et al* 2013). Accelerating warming in the Arctic and loss of sea-ice cover unfolding over the last 20 years, known as Polar or Arctic amplification (AA), raise many questions about the feedbacks of terrestrial systems coupled with the Arctic system (Serreze *et al* 2009, Screen 2014, Prowse *et al* 2015). Emerging evidence suggests that freshwater originating from the largest Arctic watersheds stimulates the AA trajectory (Yang *et al* 2014, Prowse *et al* 2015, Agafonov *et al* 2016). However, hydrology feedbacks from oceans and sea-ice on the regional basin-scale are only beginning to be recognized due to the short record length and sparse network of hydrological observations (Lammers

et al 2007, Landerer et al 2010, Shiklomanov et al 2021).

Eurasia contributes 75% of the total terrestrial runoff to the Arctic Ocean (Shiklomanov et al 2000). Large-scale reanalysis of the hydrological observations and remote sensing assessments show an accelerating rate of discharge for the large Siberian Rivers in recent decades (Syed et al 2007, Yang et al 2007, Shiklomanov et al 2021). An increase of 7% for the period 1936–1999 was first identified by Peterson et al (2002). More recent studies confirm the continuing trend of flow increase for all large rivers of the Eurasian continent and highlight a new historical maximum discharge and soil moisture water equivalent in 2007 (Shiklomanov and Lammers 2009, Tei et al 2013, Holmes et al 2016, Shiklomanov et al 2021). Climate models predict that large flow increases will continue across much of Eurasia through 2090 (Bring et al 2017). Furthermore, the winter flow displays the highest rate of increase, although this can be heavily impacted by flow regulation (Lammers et al 2001, Yang et al 2004, Magritsky et al 2018, Melnikov et al 2019). These trends are not limited to the Eurasian Arctic, as Déry et al (2016) report an 18% increase of river discharge in northern Canada over 1989–2013.

The observed recent changes in the hydrologic regime of the Arctic challenge our understanding of how streamflow responds to climate change. Studies show that intensified precipitation induced by warming climate is a major contributor to the recent rise of annual streamflow, but is not the only factor (Shiklomanov and Lammers 2009, Shiklomanov and lammers 2013). Winter streamflow appears to be particularly sensitive to increasing temperature (Wang et al 2021). Remote sensing data, used to evaluate the linkages between climate and streamflow on the sub-continental scale, reveal large differences in spatial patterns, climate variation, and forcing of permafrost thawing between basins of large Eurasian rivers, such as the Ob, Yenisei and Lena (Troy et al 2012, Wang et al 2021). The spatial distribution of permafrost in the upper reaches of these Siberian rivers varies widely, ranging from isolated (<10% of area underlain by permafrost) for the Ob River and discontinuous (50%–90%) for the Yenisei River to continuous (>90%) for the Lena River (Brown et al 2002). Most notably, the ongoing thickening of the active layer over discontinuous permafrost is contributing most to discharge anomalies (Landerer et al 2010, Makarieva et al 2019). We assume that the spatial and temporal dynamics of permafrost degradation (especially in the discontinuous zone) stimulate the permafrost driver of discharge response for climate change. Extending the record of seasonal discharge helps to gain insights to the longer range of such responses, especially in the past when climate was much cooler. A longer record would better quantify the hydrologic responses across the Arctic watersheds not only to climate change but to direct anthropogenic impacts on the terrestrial runoff as well.

The Yenisei River is the largest contributor of freshwater and energy fluxes of all Arctic rivers (Lammers et al 2007, Shiklomanov and Lammers 2013). The Yenisei River, accounting for 1.5% of global runoff, is 3487 km long, drains a 2580 000 km^2 area from Mongolia across Siberia, and empties into the Kara Sea. Tree rings can yield a long-term perspective on Yenisei River hydrology and the long-term natural variability of freshwater flux to the Kara Sea. Tree-ring data have long been useful to hydrological studies in arid regions (Schulman 1945). Yet, only recently has this potential been tested in cold regions (MacDonald et al 2007, Agafonov et al 2016, Meko et al 2020) where in some settings trees respond to air temperature variation specifically driven by water levels rather than to precipitation reflecting soil moisture stress. In this study we aim (a) to reconstruct seasonal discharge of the Yenisei River at the upper reaches situated in the discontinuous permafrost, and (b) to examine the long-term variability of the streamflow in response to climate change particularly during the winter season, when discharge trends have been pronounced.

The climate-streamflow relationship is examined with the *Water Balance/Water Transport Model (WBM)* (Grogan 2016, WSAG 2016). WBM has recently implemented a groundwater (GW) modeling algorithm (MODFLOW), which presently is the state-of-the-art GW modeling framework developed by the USGS (Hughes et al 2017). This model addition is a comprehensive hydrological system that tracks the sources and fates of water as it moves through the hydrological system including glacier melt water, snow melt, rainwater, and quantifying their relative distributions along the river systems and at any location above and below the surface (Grogan et al 2016). WBM has been applied to address a variety of hydrologic questions including global and regional water resource management and water services (Vörösmarty et al 2000, 2005), water availability and ecosystem stresses (Vörösmarty et al 2010, Shiklomanov et al 2016), permafrost impacts on hydrological conditions (Rawlins et al 2003, 2013), land use and hydrologic vulnerability (Douglas et al 2007), water temperature (Stewart et al 2013), and hydro-biochemistry (Wollheim et al 2008, 2015).

2. Methods

2.1. Yenisei river upper reaches

The Yenisei River upstream is called Ulug-Khem, a 100–650 m wide flow passing 166 km from the Kyzyl gauge down to the Sayan-Shushensky reservoir in Tuva Republic of Russian Federation. This area sits in the zone of discontinuous permafrost (Zhang

et al 2008, Wang et al 2021). The Yenisei headwaters originate at the glaciated boreal ranges of the Sayan Mountains (Tannu-Ola), yet the glacial melt contribution to the flow is negligible with respect to river discharge (Okishev 2006). The majority of glaciers (82%) in this region are smaller than 0.5 km^2 (Lucas and Gardner 2016). Snow and summer rainfall are the major sources of water at the upper reaches (35% and 42%, respectively). In terms of seasonality, the winter flow relies mainly on underground water sources, which account for 23% of the annual flow (Shiklomanov et al 2021). In Eastern Siberia, the winter flow contributes only 2%–5% of the total annual discharge while the spring-summer contribution is up to 90% (Shiklomanov et al 2021). This contrasts the Upper Yenisei system, where winter flow measures 12% of the annual discharge and persists longer, i.e. 140–150 days (Lammers et al 2007). The high flow occurs in spring (May–June) due to snowmelt beginning from mid-April. Spring discharge rapidly rises and reaches a maximum by mid-June. The snowpack is minimal in the semi desert watersheds of the Tuva trough, although the small tributaries draining the north-eastern region of the upper basin collect alpine snowmelt from the Sayan Mountains that sustains 50% of the annual flow. In mid and late summer (July–September) discharge gradually declines. However, summer floods from rainstorms may create 10–15 highwater events every year lasting 5–8 days (Serreze et al 2002). This seasonal discharge pattern is common across the Arctic watersheds with some adjustments for snowpack and permafrost conditions (Yang et al 2007, Zhang et al 2008, Wang et al 2021).

2.2. Discharge data

The Yenisei River at Kyzyl gauge represents a predominantly pristine streamflow regime without any significant regulation and water withdrawal across the watershed. The Kyzyl gauge (code 9002) is located at the confluence of two headstreams called Bolshoy Yenisei and Maliy Yenisei (or Bi-Khem and Ka-Khem in the Tuvan language). The Bolshoy Yenisei rises in the Tannu-Ola Mountain range and the Maliy Yenisei in the Darhat rift valley, Mongolia. The Kyzyl gauge is at 51.72° N, 94.40° E and 615 m asl and has a drainage area of 115 000 km^2. Seasonal dynamics of streamflow are shown in the hydrograph of figure 1, which highlights the low flow during November to April and the high flow from June to October, with the maximum discharge occurring usually in late June due to snowmelt runoff. The average annual discharge is 1025 m^3 s^{-1}. The spring flow doubles that amount (2410 m^3 s^{-1}) and in winter the flow is only about one-third of the annual average (285 m^3 s^{-1}).

The monthly observational discharge data are downloaded from the Regional Arctic Hydrographic

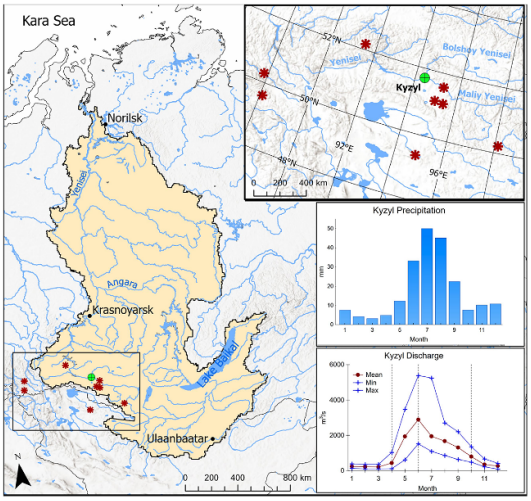

Figure 1. Map of the Yenisei River basin with locations of tree-ring sites (red) and Kyzyl gauge (green) at the upper reaches. Inserts: Topography of the upper reaches and tree-ring sites used in the discharge models (top). Bar plot of monthly precipitation from the Kyzyl weather station (1915–2019) (middle). Monthly mean (brown) and extreme (blue) discharge of the Yenisei River at Kyzyl gauge (1927–2019). Vertical dash lines outline the water seasons: low, high and summer-fall (bottom).

Network (R-ArcticNET v.4.0 www.r-arcticnet.sr.unh.edu, Lammers et al 2016). Most recent data are obtained from the State Hydrological Institute, Saint Petersburg, Russia, and have been screened for quality control via calculation of gridded runoff fields across the Arctic region (Lammers et al 2001). The Kyzyl monthly observations were updated for the 1927–2019 period, covering 92 years. Missing data are filled with linear interpolation from nearby gauges of the Yenisei River basin.

2.3. Tree-ring data

The region of interest for determining discharge history comprises the headwaters of the Yenisei River and adjacent land in the eastern ranges of the Altai Mountains where storms track and deliver precipitation to the upper reaches of the watershed (figure 1). Tree-ring data from a box bounded by the coordinates 49° N–53° N and 96° E–102° E comprises two datasets: (a) 28 tree-ring site chronologies downloaded from the International Tree-Ring Data Bank (www.ncdc.noaa.gov/data-access/paleoclimatology-data/datasets/tree-ring), and (b) 8 tree-ring chronologies from the TRISH network in Tuva (https://trish.sr.unh.edu/). The total of 36 site tree-ring chronologies were developed from cross-dated tree-ring width series of the upper and lower tree lines through the statistical procedure called standardization. Standardization optimizes the common tree-growth signal at each site by removing ring-width age-related trends and validating intervals with adequate sample size (Fritts 1976, Cook

Table 1. Statistics of tree-ring width chronologies used in the regression modeling.

Site ID	Coordinates	Elevation asl	Full interval	>0.85 EPS[a] interval	Sample size N_{trees}	Yenisei discharge correlation[b]
mong33	94.88° E, 49.37° N	2229 m	1712–1997	1712	22	−0.44
russ258	98.14° E, 50.22° N	2200 m	1700–2007	<1700	18	−0.35
russ227	88.10° E, 49.62° N	2076 m	1700–2000	<1700	24	−0.25
russ249	95.31° E, 51.58° N	2060 m	1700–2012	<1700	14	0.28*
HON	91.49° E, 52.17° N	1190 m	1783–2019	1855	22	0.28*
russ230	87.83° E, 50.27° N	1703 m	1700–2000	<1700	10	0.27*
CHG	95.45° E, 51.09° N	1035 m	1700–2017	<1700	16	−0.39
SHA	95.08° E, 51.12° N	1018 m	1700–2017	1836	17	0.33*

[a] EPS reaches 0.85 at or before (<) the indicated year.

[b] Correlation of tree-ring series with Oct–Sept or Nov–Apr average discharge at the Kyzyl gauge over 1927–1996 (70 years). Listed correlations are for discharge in year t with tree-ring index for chronologies in the reconstruction model. If predictor was lagged, correlation for with that lagged tree-ring index; lagged correlation indicated by asterisk.

and Kairiukstis 1990). Details on tree-ring chronology calculation are placed in supplementary materials (SM1 (available online at stacks.iop.org/ERL/16/125014/mmedia)). Table 1 lists statistics of the eight site chronologies used in the reconstruction models (see section 2.4). Correlation with discharge ranges from −0.44 to +0.33. The listed correlations apply to the particular lag at which the chronology is represented in the reconstruction model.

2.4. Discharge reconstruction model

Climatic signals in tree-ring chronologies are estimated with the program Seascorr (Meko *et al* 2011), which examines Pearson correlations and partial correlations between tree-ring index series and monthly data of mean temperature and precipitation aggregated over variable-length seasons (one, three and six months). The correlation analysis uses climate data from weather stations Kyzyl (RSMID#3696, 51.72° N and 94.5° E, 626 m *asl*) and Abakan (RSMID#29862, 53.77°N and 91.32°E, 254 m asl) for the interval 1925–2018, as well as CRU TS v. 4.04 0.5 degree gridded data for the interval 1901–2019 (https://climexp.knmi.nl, Harris *et al* 2020).

The statistical model selected for reconstruction was stepwise linear regression of discharge on chronologies (e.g. Woodhouse *et al* 2006). The model is problematic with just 70 observations (1927–1996) for calibration and a total of 108 potential predictors ($36 \times 3 = 108$) if even a simple lagged model with series at lags $t-1$and $t+1$ are allowed as predictors of discharge in year *t*. Protocol for statistical screening of the predictors and model verification is shown in supplementary materials (SM2). For each season, discharge between 1937 and 1996 was regressed stepwise on the 14 selected tree-ring series using p-enter = 0.25 and p-remove = 0.30 and a cross-validation stopping rule. Stepwise regression yielded the reconstruction models for seasonal and annual discharge. The first reconstruction model is

$$y = a + b_1x_1 + \ldots b_5x_5 \qquad \text{Model 1}$$

where y is the reconstructed Nov–Apr discharge in year t; $x_1, \cdots, x_5$ are tree-ring indices of mong33, russ258, and CHG in in year t, and of HON and russ230 in year $t+1$; a is the estimated regression constant; and $b_1, \ldots, b_5$ are the estimated regression coefficients. The second model is

$$y = a + b_1x_1 + \ldots b_4x_4 \qquad \text{Model 2}$$

where y is the reconstructed Oct–Sept discharge in year t;$x_1, \cdots, x_4$ are tree-ring indices of russ227 and CHG in year t, of russ249 in year $t-1$, and of SHA in year $t+1$; and the regression constant and coefficients are defined as in Model 1. While the stepwise modeling on the 14 potential predictors was restricted to the common period 1927–1996 of those chronologies, the predictors in the final models had somewhat longer common periods. Accordingly, models were re-calibrated using years 1927–1997 for Nov–Apr and 1927–2000 for Oct–Sep to arrive at models applied for long-term reconstruction.

2.5. Water balance modeling

The WBM (Grogan 2016, WSAG 2016) was used to simulate Kyzyl discharge for the same seasonal windows as the tree-ring modeling. Several WBM modules developed recently are particularly important for the Upper Yenisei. The model applies sub-grid elevation band distributions derived from a high-resolution elevation dataset (*ASTERglobal digital elevation model v2, 30 m*) where each grid cell is subdivided into several elevation bands for temperature corrections and snowmelt calculations (Lammers *et al* 1997, Hartman *et al* 1999).

WBM is also designed to use glacier model output from DEBAM or PyGEM (Lammers *et al* 2020). The exchange between GW storage and surface water hydrology is based on formulations from the USGS RIV module (MODFLOW package, Harbaugh

et al 2000, Harbaugh 2005), and simulated aquifer geometry from de Graaf *et al* (2015, 2017). The WBM was run for the 1901–2018 period in pristine mode (no human activity impacts) using monthly gridded CRU climate fields (Harris *et al* 2020). The monthly gridded climate fields for the interval 1901–2019, which are primarily based on ground observations, have been used to simulate various hydrological characteristic including runoff, discharge, soil moisture, snow accumulation, ground water storage and evapotranspiration.

3. Results

3.1. Hydrological signal of tree rings

Seascorr results for the full set of tree-ring predictors show that climatic impact on conifer tree growth is relatively coherent in these semi-arid regions despite the diverse topography and tree ecology. In general, moisture from precipitation stimulates tree growth, while high temperature promotes evapotranspiration and creates drought stress and smaller rings (Meko *et al* 1995, Panyushkina *et al* 2018). Yet, the physiological mechanism behind larch tree-ring growth response to climate at the site level is not fully understood. Moreover, the available climate data are sparse, and cannot be expected to match well with the precipitation history at the tree sites. Local precipitation is also to some extent influenced by altitude, position, exposure, and aspect of mountain ridges. It is therefore encouraging that, despite these limitations, we find broadly consistent patterns of correlation of chronologies with seasonal climate variables. For *Larix* in this region, a recurring pattern is positive correlation of ring widths with summer temperature (predominantly June) that regulates the growth rate (e.g. cell division and arrangement) at the beginning of growth season (Panyushkina *et al* 2003, Belokopytova *et al* 2018).

Figure S1 shows correlation patterns larch ring growth with climate. While there are no studies of larch cambial phenology at the Yenisei upper reaches, the timing of larch wood formation in Khakassia and larch physiological traits in Tuva are most likely similar. Khakassia is about 350 km downstream from Kyzyl, the closest region, where the impact of hydroclimate variations on larch physiology has been studied (Fonti and Babushkina 2016, Belokopytova *et al* 2018, Shiklomanov *et al* 2021). Larch ring growth at the upper tree line normally begins in early June, and two weeks earlier at the lower tree line. Larch growth enters a dormant phase in September. Most importantly, the climatic signal is recorded in xylem formation throughout the entire growth season, May–September (Belokopytova *et al* 2018).

The calculated response is explained by the limiting role of both temperature and precipitation on the soil moisture and hydrological regime. The relationship between air temperature and tree-growth is critical to the reconstruction of Yenisei River discharge and complimentary to the precipitation-sensitive growth. Climatically comparable growth conditions over much of the vegetation period are commonly reported for a broad range of geographical droughts (Alan *et al* 2019). Depleted reserves of soil water restrict trees from profiting from the warm temperature in spring /early summer and consequently their radial growth shows a reduction (Scharnweber *et al* 2020). This compensation mechanism highlights the pivotal role of soil water recharge and lag effects in the regression modeling (Meko *et al* 1995, 2007). Table 1 indicates significant correlation of discharge variations from year to year with the tree-ring chronologies used as the predictants. The correlations are negative with growth of the current year and positive with the subsequent (lagged) year. Larch growth is commonly reduced in high-flow years and increased in low-flow years (Agafonov *et al* 2016).

3.2. Seasonal discharge reconstruction

Generating a reconstruction from the selected predictor pool was also successful. Both models demonstrate skill in prediction since the reduction of error (RE) statistic is positive in both cases (table 2). There was no indication the model residuals violated any assumptions, as indicated by a non-significant DW statistic (table 2), a normal-looking histogram, and a featureless scatterplot of residuals on fitted values (figure S2). Moreover, a straight line fit of residuals against time indicated no significant trend in residuals. Supplementary materials include the equations of the two reconstructed models: Nov–Apr low water season and annual discharge of Oct–Sept (equations S1 and S2).

Stepwise regression of the selected tree-ring chronologies with Yenisei discharge at the Kyzyl gauge finds two seasonal groupings: (a) a 6 month period beginning in November of the preceding growth year and ending in the following April with the strongest signal ($R^2 = 0.52$, F = 14.14, $p < 0.00001$) (table 2), and (b) a 12 month window beginning in October of the preceding growth year with a weaker signal ($R^2 = 0.26$, $F = 6.08$, $p < 0.001$). Although the signal of the second seasonal grouping was weaker, it is still comparable with signals obtained for the Ob River basin from the Eurasian pan-Arctic (Agafonov *et al* 2016, Meko *et al* 2020). Both signals are sufficiently strong to justify the reconstruction effort.

The developed Nov–Apr tree-ring reconstruction tracks the year-to-year variations of baseflow discharge and water-year discharge since 1784. The decadal and multidecadal variability of the two reconstructed flow series is similar and the reconstructions share common features until 1960, after which the

Table 2. Reconstruction statistics for Yenisei River streamflow at the Kyzyl gauge. Calibration interval: 1927–1997 (71 years) in Model #1 and 1927–2000 (74 years) in Model #2.

Predictant	Predictors	R	R^2	adjR^2	DW	F	RE	RMSEcv
Model #1 Nov–Apr	mong33$_t$ russ258$_t$ CHG$_t$ HON$_{t-1}$ russ230$_{t+1}$	0.72	0.52	0.48	1.94 ($p = 0.54$)	14.14 $df = (5, 65)$ $p <$ 1E-8	0.44	41.2832
Model #2 Oct–Sept	russ227$_t$ CHG$_t$ russ249$_{t-1}$ SHA$_{t+1}$	0.51	0.26	0.22	1.85 ($p = 0.40$)	6.08 $df = (4, 69)$ $p < 0.001$	0.11	126.3911

[a] R—coefficient of correlation; R^2—coefficient of determination; adjR^2—coefficient of determination adjusted for number of predictors in model; RE—cross-validation reduction of error; DW—Durbin-Watson statistic and its p-value ($p > 0.05$ indicates no lag-1 autocorrelation of residuals); F-overall F-statistic for testing significance of regression model, with degrees of freedom and p-value ($p < 0.05$ indicates significant model); RMSEcv—root-mean-square error of cross-validation, a measure of reconstruction uncertainty.

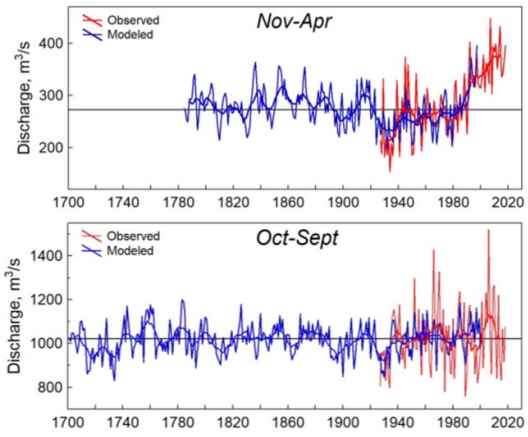

Figure 2. Reconstructed Nov–Apr (top) and Oct–Sept (bottom) discharge of the Yenisei River (blue line). Red line is the instrumental flow at the Kyzyl gauge (1927–2019). The thick line is the 10 year moving average. Horizontal line is the gauged mean.

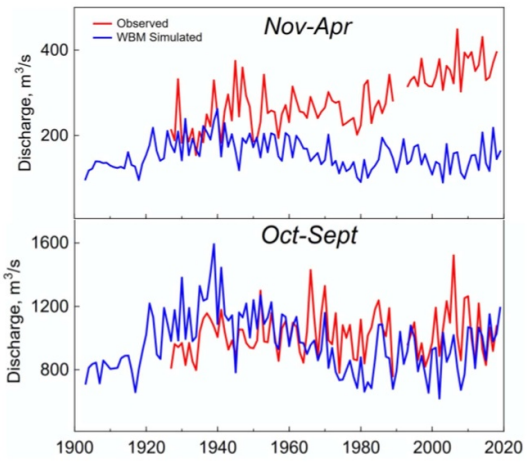

Figure 3. Observed and WBM simulated Nov–Apr and Oct–Sept seasonal discharge of the Yenisei River at Kyzyl gauge. WBM simulated discharge derived from CRU climate drivers. Table S2 shows the model statistics.

agreement falls apart. In particular, the rate of flow in the winter has accelerated considerably over the last 25 years. The winter flow had a prolonged 71 year period (1920–1990) below the historical mean, then suddenly surged up (figure 2, Nov–Apr). The annual flow rises in 1960–1970 then gradually declines over the next decade, stays elevated during 1995–2015 and finally declines again until the present (figure 2, Oct–Sept).

Discharge modeled with tree-rings is double the length of the instrumental record at the Upper Yenisei and found (a) the unprecedented upsurge of baseflow from 1995 and (2) a significant disagreement in the rate and trend of fluctuations between the winter and annual flow during 1995–2019.

3.3. Water balance modeling of discharge

The streamflow–climate relationships for two seasonal windows were evaluated using long-term simulations with the water-balance model (WBM at the Upper Yenisei basin for the interval 1905–2019, 114 years). WBM results show high sensitivity of discharge to precipitation and temperature that tracks well the decadal and multidecadal variability of the flow while systematically underestimating the annual variance (figure 3 and table S2). This could be caused by underestimation of precipitation in our input climate dataset especial in the early observations (figure S3), which may poorly represent the high-elevation precipitation pattern. The number of meteorological stations is sparse, and precipitation varies extensively in space in the Sayan Mountains. Moreover, WBM probably does not consider some environmental factors and processes that may regularly contribute to the discharge variance at annual and seasonal scales. For example, due to insufficient climate and land cover data over such a long period, we had to use simplified evapotranspiration calculations and ignore glacier melt and permafrost thaw. This neglects the possible role of permafrost degradation in the recent increase of the flow.

Another notable feature of the WBM calculated series is a significant increase of the estimate error in the winter discharge after 1960 (figure 3, Oct–Sept). The climate drivers decreased their rate of change during 1960–2000 while the baseflow continued accelerating higher. It appears the winter flow decoupled from the decadal trends in climate variability during that time. This large discrepancy in the WBM simulated and observed discharge suggests that the feedbacks of the main forcing factors input to the WBM altered over the period 1960–2000. However, the climate–winter flow relationship strengthened after 2000 and the simulated variance closed the gap with the instrumental flow.

4. Discussion

Tree-ring reconstruction of seasonal discharge for the Upper Yenisei extends the instrumental record of winter flows at Kyzyl from 1927 back to 1784. This is the first and only reconstructed winter flow in the Siberian region, bringing a new perspective to streamflow dynamics. The reconstruction permits analysis of both the long-term (decadal and multidecadal) and annual variability of discharge. The long-term variability of winter flow differs significantly from the annual flow. The reconstruction finds a remarkable 80% upsurge of the winter discharge over the last 25 years that is unprecedented in the last 235 years, while the annual discharge increases by only 7%. Our reconstructed annual flow corresponds very well to an independently produced tree-ring reconstruction of Selenga River discharge for the interval 1708–1998 (Andreev *et al* 2016), which also derives part of its flows from precipitation in the mountainous upper headwaters of Altai-Sayan Mountains as well as from arid parts of the Yenisei Basin southeast of Lake Baikal in Mongolia (figure S4).

Many studies generally attribute the recent change of flow rate across the Eurasian pan Arctic to warming air temperature, seasonal changes of precipitation, or snowpack dynamics (Yang *et al* 2003, 2007, McClelland *et al* 2004, Wu *et al* 2005, Zhang *et al* 2018). However, more recent assessments conclude that the primary driver of the flow change is enhancement of regional surface–groundwater interactions due to degradation of the permafrost (Evans *et al* 2020). The linear regression slope of air temperature fields (CRU T.4, 1905–2019) is positive overall at the upper reaches of the Yenisei since 1960s (figure S5). Figure S6 shows a positive linear regression slope in active layer depth data for the interval 2000–2018. CRU reanalysis addressed the studied watersheds, finding no extraordinary changes in seasonal pattern of summer temperature after 1960 and 1995 (figure S7). Tree-ring reconstructions of summer temperature and precipitation across the Altai-Sayan Mountains suggest that the rate of precipitation and temperature change in the late 20th century is not unusual in the context of the last 300 years. The late 20th century was relatively cool and wet and the most recent decades warm and dry (Myglan *et al* 2012, Kostyakova *et al* 2018, Fedotov *et al* 2019, Oyunmunkh *et al* 2019). Strong correspondence of river discharge to seasonal snow cover changes does not fully explain the winter flow rate (Yang *et al* 2007, Troy *et al* 2012). Studies covering various time periods show snow cover and snow depth decreased in the studied region between 1936–2007 (Ye *et al* 1998, Bulygina *et al* 2009). VIC-simulated seasonal runoff for the interval 1936–1999 indicates opposite trends in snowpack variability between the north and south Yenisei River basin with significant reduction of snowpack in the south (Troy *et al* 2012). It is evident that neither temperature, seasonal precipitation changes, nor snowpack dynamics are the primary drivers of the documented streamflow change.

It is worth mentioning the role increased fire frequency plays on the degradation of permafrost. Carbon emission modeling finds Siberia to be an increasingly significant region where frequent boreal fires and intense large area burns impact climate and permafrost (Conard *et al* 2002, Soja *et al* 2004a, Tchebakova *et al* 2009, Kukavskaya *et al* 2016 , Gibson *et al* 2018, Biskaborn *et al* 2019). Smoke plumes from south Siberian fires (including the Sayan Mountains, especially near Lake Baikal) have been noticeable on the global scale since the late 1990s (Warneke *et al* 2009). Soja *et al* (2004b) report on the post-fire impact on the seasonal frozen layer and soil temperature dynamics. After forest fire, soil temperature can increase by as much as 2 °C–6 °C for up to 15 years after the fire, which, as has been observed since the mid-20th century, also increases the depth of permafrost thaw (Kershaw *et al* 1975, Viereck and Schandelmeier 1980, Van Cleve and Viereck 1983, Furyaev 1996, O'Neill *et al* 2003, Kirdyanov *et al* 2020). In connection with forest fires, ground-based data estimates the top of permafrost is subsiding at a rate of 0.52 cm yr^{-1} in the Yenisei River Basin (Knorre *et al* 2019). Overall, the increased fire frequency in southern Siberia likely impacts the aquifer level in the discontinuous permafrost and the water-storing capacity of the ground, which enhances ground water discharge to the flow.

Climatologically, the frequent fires over arid south Siberia are linked to a local high-pressure system controlled by the Arctic Oscillation (Kim *et al* 2020). Anomalous warmth in late winter (0.8 °C–1.2 °C in Feb–March) enhances evaporation, causing earlier ground surface exposure and drier ground in spring that promotes the spread of fire. AA, due to the weakening of midlatitude jets, is linked to the weather patterns that increase the probability of extreme weather in the study region (Cohen *et al* 2014, Screen 2014). Interestingly, increased flows is both a consequence of AA, due to the same process described above, and

a contributor to AA as larger winter flows bring significantly more fresh water to the Kara Sea.

We hypothesize that the recent upsurge in winter flow resulted from melting permafrost, which itself is a consequence of a warming climate. The lack of long-term studies on permafrost degradation at the upper reaches of the Yenisei River complicates our understanding of permafrost's impact on the hydrological regime (Walvoord and Kurylyk 2016). Still, multiple lines of evidence suggest permafrost plays a key role in this upsurge of winter flows. Biskaborn *et al* (2019) report accelerating permafrost warming in the circumpolar Arctic in the last decade of up to 0.20 ± 0.10 °C in the discontinuous zone. Large-scale satellite gravitational measurements (GRACE) of the Eurasian pan-Arctic water budget attribute the thickening of the active layer to melting ground ice in discontinuous permafrost, directly contributing to the changes of river discharge since 2003 (Landerer *et al* 2010). Park *et al* (2016) showed long-term regional trends (1980–2009) of 0.03 m −0.06 m decade $^{-1}$ in thickness of the active layer over the permafrost extent, indicating widespread permafrost degradation. Measurements of stable isotope composition of Yenisei water in watersheds with degraded permafrost show that winter flow decouples from the precipitation isotopic signature in the 21st century (Streletskiy *et al* 2015). Active-layer depth over Siberia steadily increased over 1956–1990 (Frauenfeld *et al* 2004, Zhang *et al* 2005) and continued increasing into the 2000s (Luo *et al* 2016). Finally, the most recent remote sensing data report a rate of 4.4 mm per year over 1980–2016 in thickening of the active layer across Siberia, which increased the storage capacity of discontinuous permafrost and the contribution of ground water to river discharge during the winter months (Wang *et al* 2021).

These changes have implications for the vegetation that grows there. The boundary between the active layer and permafrost plays an important role as source water storage (Sugimoto *et al* 2003). Late-summer-fall precipitation infiltrates into the seasonally frozen layer and mixes with ice-thaw water. The impact of increased evaporation of surface water on Eastern Siberian streamflow is not significant (Sugimoto and Maximov 2012), meaning that ongoing thickening of the active layer due to warming spring temperatures implies thermal distress during growth onset.

A warm spring prompts rapid snowmelt, cooler soil temperature and excess moisture, delaying the onset of growth (Agafonov *et al* 2016, Kannenberg *et al* 2019). Furthermore, the positive correlation of tree growth with previous summer and fall precipitation suggests that the growth rate of the current year is enhanced by soil-water recharge during the previous fall, the lack of which can limit accumulation of non-structural carbohydrates that provide reserves necessary for spring growth (Choat *et al* 2018).

5. Conclusion

Tree-ring proxies of summer temperature and precipitation define the linkage between climate and Yenisei streamflow. Regression of tree-ring width series with discharge is useful for reconstructing seasonal streamflow changes over centuries in arctic watersheds. Tree ring widths account for 52% to 27% of the explained variance of seasonal and annual flow of the Yenisei River. Applying tree rings from high and low elevations allows modeling of at least two, and possibly more, water seasons from a single watershed. Further efforts should be focused toward increasing the sample depth of the tree-ring chronologies to extend the interval of reconstructed flow dynamics back in time. Reconstruction of the Upper Yenisei flow found an unprecedented increase in the winter flow rate between 1995 and 2019, which is not seen in the record going back to 1784. This rate is nearly 80% above the instrumental and reconstructed average. Water balance modeling indicates the weakening of climate and streamflow linkages soon after 1960. Many studies link AA with the intensified degradation of discontinuous permafrost and boreal forest fires, possibly driving the change of winter flow rate in recent decades.

Data availability statement

The data that support the modeling and findings of this study are available from the corresponding author or the University of Arizona Library (https://doi.org/10.25422/azu.data.17086889).

All data that support the findings of this study are included within the article (and any supplementary files).

Acknowledgments

The study is part of the Tree-Ring Integrated System for Hydrology (TRISH project) that is supported by funding from U.S. NSF Polar Office program #1917503 and #1917515. We also acknowledge support from the Russian Science Foundation (RSF) #19-14-00028 to V Myglan. We thank Professor Orlan Oidupaa (Tuva State University) for the generous assistance in the field, and Alec C Gagliano and Misha Seroukhov (students of University of Arizona) for the lab assistance.

Author contribution

I P P conceptualized the study, developed the tree-ring datasets, modeled and analyzed the Yenisei discharge, and wrote the manuscript. D M assisted in computer programming, modeling and in editing the draft. A S H provided hydro-climatic instrumental data and simulated W B M series. R T discussed and

edited the draft, helped with figures drawings. V M, V V B and A V T collected the tree ring samples in Tuva and crossdated the tree-ring materials from S T A and C H G sites.

ORCID iDs

Irina P Panyushkina https://orcid.org/0000-0001-8854-2637
Alexander Shiklomanov https://orcid.org/0000-0001-9790-3510

References

Aagaard K and Carmack E C 1989 The role of sea ice and other fresh water in the Arctic circulation *J. Geophys. Res.* **94** 14485–98

Agafonov L I, Meko D and Panyushkina I P 2016 Reconstruction of Ob River, Russia, from ring widths of floodplain trees *J. Hydrol.* **543** 198–217

Allen S T, Kirchner J W, Braun S, Siegwolf R T W and Goldsmith G R 2019 Seasonal origins of soil water used by trees *Hydrol. Earth Syst. Sci.* **23** 1199–210

Andreev S G, Garmaev E J, Ayurzhanaev A A, Batotsyrenov E A and Gurzhapov B O 2016 Reconstructed runoff and historical archives of the extreme weather events in the Baykal Asia *Guigoz Sci. Rev.* **5** 35–38

Belokopytova L V, Babushkina E A, Zhirnova D F, Panyushkina I P and Vaganov E A 2018 Pine and larch tracheidograms capture seasonal variations of climatic signal at moisture-limited site *Trees* **33** 227–42

Biskaborn B K *et al* 2019 Permafrost is warming at a global scale *Nat. Commun.* **10** 264–78

Bring A, Shiklomanov A and Lammers R B 2017 Pan-Arctic river discharge: prioritizing monitoring of future climate change hot spots *Earth's Future* **5** 72–92

Brown J, Ferrians O J, Heginbottom J A and Melnikov E 2002 *Circum-Arctic Map of Permafrost and Ground Ice Conditions, Version 2* (Boulder, CO: NSIDC: National Snow and Ice Data Center) (1 May 2021) (https://doi.org/10.7265/skbg-kf16)

Bulygina O N, Razuvaev V N and Korshunova N N 2009 Changes in snow cover over Northern Eurasia in the last few decades *Environ. Res. Lett.* **4** 045026

Choat B, Brodribb T J, Brodersen C R, Duursma R A, López R and Medlyn B E 2018 Triggers of tree mortality under drought *Nature* **558** 531–9

Cohen J *et al* 2014 Recent Arctic amplification and extreme mid-latitude weather *Nat. Geosci.* **7** 627–63

Conard S G, Sukhinin A I, Stocks B J, Cahoon D R Jr, Davidenko E P and Ivanova G A 2002 Determining effects of area burned and fire severity on carbon cycling and emissions in Siberia *Clim. Change* **55** 197–211

Cook E R and Kairiukstis L A 1990 *Methods of Dendrochronology: Applications in the Environmental Sciences* (Dordrecht: Kluwer Academic Publishers)

de Graaf I E M, Sutanudjaja E H, van Beek L P H and Bierkens M F P 2015 A high-resolution global-scale groundwater model *Hydrol. Earth Syst. Sci.* **19** 823–37

de Graaf I E M, van Beek R L P H, Gleeson T, Moosdorf N, Schmitz O, Sutanudjaja E and Bierkens M F P 2017 A global-scale two-layer transient groundwater model: development and application to groundwater depletion *Adv. Water Resour.* **102** 53–67

Déry S J, Stadnyk T A, MacDonald M K and Gauli-Sharma B 2016 Recent trends and variability in river discharge across northern Canada *Hydrol. Earth Syst. Sci.* **20** 4801–18

Douglas E M, Wood S, Sebastian K and Vorosmarty C J 2007 Policy implications of a pan-tropic assessment of the simultaneous hydrological and biodiversity impacts of deforestation *Water Resour. Manage.* **21** 211–32

Evans S G, Yokeley B, Stephens C and Brewer B 2020 Potential mechanistic causes of increased baseflow across northern Eurasia catchments underlain by permafrost *Hydrol. Process.* **34** 2676–90

Fedotov P, Enushchenko I V and Zheleznyakova T O 2019 Reconstruction of climate changes in East Siberia (Russia) from 1500 AD to the present based on tree-rings records *Int. J. Environ. Stud.* **76** 266–72

Fichot C G, Kaiser K, Hooker S B, Amon R M W, Babin M, Belanger S, Walker S A and Benner R 2013 Pan-Arctic distributions of continental runoff in the Arctic ocean *Nat. Sci. Rep.* **3** 1053

Fonti P and Babushkina E A 2016 Tracheid anatomical responses to climate in a forest-steppe in Southern Siberia *Dendrochronologia* **39** 32–41

Frauenfeld O W, Zhang T, Barry R G and Gilichinsky D 2004 Interdecadal changes in seasonal freeze and thaw depths in Russia *J. Geophys. Res.* **109** D5

Fritts H C 1976 *Tree Rings and Climate* (London: Academic Press)

Furyaev V V 1996 Pyrological regimes and dynamics of the southern Taiga forests in Siberia *Fire in Ecosystems of Boreal Eurasia* vol 48, ed J G Goldammer and V V Furyaev (Dordrecht: Kluwer Academic Publishing) 168–85

Gibson C M, Chasmer L E, Thompson D K, Quinton W L, Flannigan M D and Olefeldt D 2018 Wildfire as a major driver of recent permafrost thaw in boreal peatlands *Nat. Commun.* **9** 3041

Grogan D S 2016 Global and regional assessments of unsustainable groundwater use in irrigated agriculture *PhD Thesis* University of New Hampshire

Harbaugh A W 2005 MODFLOW-2005, the U.S. geological survey modular ground-water model—the ground-water flow process (*U.S. Geological Survey Techniques and Methods* 6-A16) (available at: https://pubs.usgs.gov/tm/2005/tm6A16/)

Harbaugh A W, Banta E R, Hill M C and McDonald M G 2000 MODFLOW-2000 U.S. geological survey modular ground-water model—user guide to modularization concepts and the ground-water flow process (*U.S. Geological Survey Open-File Report* 00–92)

Harris I, Osborn T J, Jones P and Laster D 2020 Version 4 of the CRU TS monthly high-resolution gridded multivariate climate dataset *Sci. Data* **7** 109

Hartman M D, Baron J S, Lammers R B, Cline D W, Band L E, Liston G E and Tague C 1999 Simulations of snow distribution and hydrology in a mountain basin *Water Resour. Res.* **35** 1587–603

Holmes R M, Shiklomanov A I, Tank S E, McClelland J W and Tretiakov M 2016 River discharge *Bull. Am. Meteorol. Soc.* **97** S147–149

Hughes J D, Langevin C D and Banta E R 2017 Documentation for the MODFLOW 6 framework *U.S. Geological Survey Techniques and Methods* 6 A57 p 40

Kannenberg S A, Maxwell J T, Pederson N, D'Orangeville L, Ficklin D L and Phillips R P 2019 Drought legacies are dependent on water table depth, wood anatomy and drought timing across the eastern US *Ecol. Lett.* **22** 119–27

Kershaw K A, Rouse W R and Bunting B T 1975 The impact of fire on forest and tundra ecosystems. *Arctic Land Use Res. Progra, Dept. Indian Affairs and N. Develop. Ottawa. North of 60. ALUR Rept.* 74–75-63

Kim J-S, Kug J-S, Jeong S-J, Park H and Schaepman-Strub G 2020 Extensive fires in southeastern Siberian permafrost linked to preceding Arctic Oscillation *Sci. Adv.* **6** eaax330

Kirdyanov A V, Saurer M, Siegwolf R, Knorre A A, Prokushkin A S, Churakova (Sidorova) O V, Fonti M V and Büntgen U 2020 Long-term ecological consequences of forest fires in the continuous permafrost zone of Siberia *Environ. Res. Lett.* **15** 034061

Knorre A A, Kirdyanov A V, Prokushkin A S, Krusic P J and Büntgen U 2019 Tree ring-based reconstruction of the

long-terminfluence of wildfires on permafrost active layer dynamics in Central Siberia *Sci. Total Environ.* **652** 314–9
Kostyakova T V, Touchan R, Babushkina E A and Belokopytova L 2018 Precipitation reconstruction for the Khakassia region, Siberia, from tree rings *Holocene* **28** 377–85
Kukavskaya E A, Buryak L V, Shvetsov E G, Conard S G and Kalenskaya O P 2016 The impact of increasing fire frequency on forest transformations in southern Siberia *For. Ecol. Manage.* **382** 225–35
Lammers R B, Band L E and Tague C L 1997 Scaling behaviour of watershed processes *Scaling-up* ed P van Gardingen, G Foody and P Curran (Cambridge: Cambridge University Press) pp 295–317
Lammers R B, Pundsack L W and Shiklomanov A I 2007 Variability in river temperature,discharge, and energy flux from the Russian pan-Arctic landmass *J. Geophys. Res.* **112** G04S59
Lammers R B, Shiklomanov A I, Vörösmarty C J, Fekete B M and Peterson B J 2001 Assessment of contemporary Arctic river runoff based on observational discharge records *J. Geophys. Res.* **106** 3321–34
Lammers R B, Shiklomanov A I, Vörösmarty C J, Fekete B M and Peterson B J 2016 R-ArcticNet, A regional hydrographic data network for the Pan-Arctic Region (ISO-image of CD-ROM) *PANGAEA* (https://doi.org/10.1594/PANGAEA.85942)
Landerer F W, Dickey J O and Güntner A 2010 Terrestrial water budget of the Eurasian pan-Arctic from GRACE satellite measurements during 2003–2009 *J. Geophys. Res.* **115** D23115
Lucas E and Gardner A 2016 A satellite-derived glacier inventory for North Asia *Ann. Glaciol.* **57** 50–60 Interdecadal changes in seasonal freeze and thaw depths in Russia *J. Geophys. Res.* **109** D05101
Luo D, Wu Q, Jin H, Marchenko S S, Lu L and Gao S 2016 Recent changes in the active layer thickness across the northern hemisphere *Environ. Earth Sci.* **75** 555
MacDonald G M, Kremenetski K V, Smith L C and Hidalgo H G 2007 Recent Eurasian river discharge to the Arctic Ocean in the context of longer- term dendrohydrological records *J. Geophys. Res.* **112** G04S50
Magritsky D V, Frolova N L, Evstigneev V M, Povalishnikova E S, Kireeva M B and Pakhomova O M 2018 Long-term changes of river water inflow into the seas of the Russian Arctic sector *Polarforschung* **87** 177–94
Makarieva O, Nesterova N, Post D A, Sherstyukov A and Lebedeva L 2019 Warming temperatures are impacting the hydrometeorological regime of Russian rivers in the zone of continuous permafrost *Cryosphere* **13** 1635–59
McClelland J W, Holmes R M, Peterson B J and Stieglitz M 2004 Increasing river discharge in the Eurasian Arctic: consideration of dams, permafrost thaw, and fires as potential agents of change *J. Geophys. Res.* **109** D18102
Meko D M, Panyushkina I P, Agafonov L I and Edwards J A 2020 Impact of high flows of an Arctic river on ring widths of floodplain trees *Holocene* **30** 789–98
Meko D M, Stockton C W and Boggess W R 1995 The tree-ring record of severe sustained drought *J. Am. Water Resour. Assoc.* **31** 789–801
Meko D M, Touchan R and Anchukaitis K A 2011 Seascorr: a MATLAB program for identifying the seasonal climate signal in an annual tree-ring time series *Comput. Geosci.* **37** 1234–41
Meko D, Woodhouse C A, Baisan C A, Knight T, Lukas J J, Hughes M K and Salzer M W 2007 Medieval drought in the upper Colorado River Basin *Geophys. Res. Lett.* **34** L10705
Melnikov V P, Pikinerov P V, Gennadinik V B, Babushkin A G and Moskovchenko D V 2019 Change in the hydrological regime of Siberian rivers as an indicator of changes in cryological conditions *Dokl. Earth Sci.* **487** 990–4
Myglan V S, Zharnikova O A, Malysheva N V, Gerasimova O V, Vaganov E A and Sidorova O V 2012 Constructing tree-ring chronology and reconstructing summertime air temperatures in southern Altai for the last 1500 years *Geogr. Nat. Resour.* **33** 200–7
O'Neill K P, Kasischke E S and Richter D D 2003 Seasonal and decadal patterns of soil carbon uptake and emission along an age sequence of burned black spruce stands in interior Alaska *J. Geophys. Res.* **108** 8155
Okishev P A 2006 Topography and glaciation Russian Altai *Problems of Geography of Siberia* ed P A Okishev and J K Narozhnyi (Tomsk: Tomsk University Press) pp 39–55
Oyunmunkh B, Weijers S, Loeffler J, Byambagerel S, Soninkhishig N, Buerkert A, Goenster-Jordan S and Simme C 2019 Climate variations over the southern Altai Mountains and Dzungarian Basin region, Central Asia, since 1580 CE *Int. J. Climatol.* **39** 4543–58
Panyushkina I P, Hughes M K, Vaganov E A and Munro M A R 2003 Summer temperature in northeastern Siberia since 1642 reconstructed from tracheid dimensions and cell numbers of Larix cajanderi *Can. J. For. Res.* **33** 1905–14
Panyushkina I P, Meko D M, Macklin M G, Toonen W H J, Mukhamedeiv M M, Konovalov V G, Ashikbaev N Z and Sagitov A O 2018 Runoff variations in Lake Balkhash Basin, Central Asia, 1779–2015 inferred from tree rings *Clim. Dyn.* **51** 3161–77
Park H, Kim Y and Kimball J S 2016 Widespread permafrost vulnerability and soil active layer increases over the high northern latitudes inferred from satellite remote sensing and process model assessments *Remote Sens. Environ.* **175** 349–58
Peterson B J, Holmes R M, McClelland J W, Vörösmarty C J, Lammers R B, Shiklomanov A I, Shiklomanov I A and Rahmstorf S 2002 Increasing river discharge to the Arctic Ocean *Science* **298** 2171–3
Prowse T, Bring A, Mård J, Carmack E, Holland M, Instanes A, Vihma T and Wrona F J 2015 Arctic Freshwater Synthesis: summary of key emerging issues *J. Geophys. Res. Biogeosci.* **120** 1887–93
Rahmstorf S 2002 Ocean circulation and climate during the past 120,000 years *Nature* **419** 207–14
Rawlins M A, Lammers R B, Frolking F, Fekete B M and Vorosmarty C J 2003 Simulating pan- arctic runoff with a macro-scale terrestrial water balance model *Hydrol. Process.* **17** 2521–39
Rawlins M D, Nicolsky J, McDonald K and Romanovsky V E 2013 Simulating soil freeze/thaw dynamics with an improved Pan-Arctic water balance model *J. Adv. Model. Earth Syst.* **5** 1–17
Rencher A C and Pun F C 1980 Inflation of R2 in best subset regression *Technometrics* **22** 49–53
Rounce D R, Hock R and Shean D E 2020 Glacier Mass Change in High Mountain Asia Through 2100 Using the Open-Source Python Glacier Evolution Model (PyGEM) *Front. Earth Sci.* **7** 331
Scharnweber T, Smiljanic M, Cruz-García R, Manthey M and Wilmking M 2020 Tree growth at the end of the 21st century—the extreme years 2018/19 as template for future growth conditions *Environ. Res. Lett.* **15** 074022
Schulman E 1945 Tree-ring hydrology of the Colorado River Basin *Univ. Arizona Bull.* **16** 1–51
Screen J A 2014 Arctic amplification decreases temperature variance in northern mid- to high-latitudes *Nat. Clim. Change* **4** 577–82
Serreze M C, Barrett A P, Stroeve J C, Kindig D N and Holland M M 2009 The emergence of surface-based Arctic amplification *Cryosphere* **3** 11–19
Serreze M C, Bromwich D H, Clark M P, Etringer A J, Zhang T and Lammers R B 2002 The large scale-hydro-climatology of the terrestrial arctic drainage system *J. Geophys. Res.* **107** ALT 1-1-ALT 1–28
Shiklomanov A I and Lammers R B 2009 Record Russian river discharge in 2007 and the limits of analysis *Environ. Res. Lett.* **4** 045015

Shiklomanov A I and Lammers R B 2013 Changing discharge patterns of high-latitude Rivers *Clim. Vulnerability* **5** 161–75
Shiklomanov A, Déry S, Tretiakov M, Yang D, Magritsky D, Georgiadi A and Tang W 2021 River freshwater flux to the Arctic Ocean *Arctic Hydrology, Permafrost and Ecosystems* ed D Yang and D L Kane (Berlin: Springer) pp 703–8
Shiklomanov A, Prusevich A, Gordov E, Okladnikov I and Titov A 2016 Environmental science applications with rapid integrated mapping and analysis system (RIMS) *IOP Conf. Series Earth and Environmental Science* vol 48 pp 012034
Shiklomanov I A, Shiklomanov A I, Lammers R B, Peterson B J and Vörösmarty C J 2000 The dynamics of river water inflow to the Arctic Ocean *The Freshwater Budget of the Arctic Ocean* vol 70, ed E L Lewis, E P Jones, P Lemke, T D Prowse and P Wadhams (Berlin: Springer) pp 281–96
Soja A J, Cofer W R, Shugart H H, Sukhinin A I, Stackhouse J P W, McRae D J and Conard S G 2004a Estimating fire emissions and disparities in boreal Siberia (1998–2002) *J. Geophys. Res.* **109** D14S06
Soja A J, Sukhinin A I, Cahoon Jr J D R, Shugart H H and Stackhouse Jr J P W 2004b AVHRR-derived fire frequency, distribution and area burned in Siberia *Int. J. Remote Sens.* **25** 1939–60
Stewart R J, Wollheim W M, Miara A, Vörösmarty C J, Fekete B, Lammers R B and Rosenzweig B 2013 Horizontal cooling towers: riverine ecosystem services and the fate of thermoelectric heat in the contemporary *Environ. Res. Lett.* **8** 025010
Streletskiy D, Tananaev N, Opel T, Shiklomanov N, Nyland K, Streletskaya I, Tokarev I and Shiklomanov A 2015 Permafrost hydrology in changing climatic conditions: seasonal variability of stable isotope composition in rivers in discontinuous permafrost *Environ. Res. Lett.* **109** 095003
Sugimoto A and Maximov T C 2012 Study on hydrological processes in Lena River Basin using Stable Isotope ratios of River water IAEA (available at: www-pub.iaea.org/MTCD/Publications/PDF/TE_1673_Web.pdf)
Sugimoto A, Naito D, Yanagisawa N, Ichiyanagi K, Kurita N, Kubota J, Kotake T, Ohata T, Maximov T C and Fedorov A N 2003 Characteristics of soil moisture in permafrost observed in East Siberian taiga with stable isotopes of water *Hydrol. Process.* **17** 1073–92
Syed T H, Famiglietti J S, Zlotnicki V and Rodell M 2007 Contemporary estimates of Pan-Arctic freshwater discharge from GRACE and reanalysis *Geophys. Res. Lett.* **34** L19404
Tchebakova N M, Parfenova E and Soja A J 2009 The effects of climate, permafrost and fire on vegetation change in Siberia in a changing climate *Environ. Res. Lett.* **4** 045013
Tei S, Sugimoto A, Yonenobu H, Yamazaki T and Maximov T C 2013 Reconstruction of soil moisture for the past 100 years in eastern Siberia by using δ13 C of larch tree rings *J. Geophys. Res. Biogeosci.* **118** 1256–65
Troy T J, Sheffield J and Wood E F 2012 The role of winter precipitation and temperature on northern Eurasian streamflow trends *J. Geophys. Res.* **117** D05131
Van Cleve K and Viereck L A 1983 A comparison of successional sequences following fire on permafrost-dominated and permafrost-free sites in interior Alaska *Permafrost: Proc. of the Fourth Int. Conf.* (National Academy) pp 1286–91 (www.arlis.org/docs/vol1/ICOP/10368063.pdf)
Viereck L A and Schandelmeier L H 1980 *Effects of Fire in Alaska and Adjacent Canada—A Literature Review Anchorage* (Alaska: U.S. Dept. of the Interior, Bureau of Land Management, Alaska State Office) (www.arlis.org/susitnadocfinder/Record/92011)
Vörösmarty C J *et al* 2010 Global threats to human water security and river biodiversity *Nature* **467** 555–61
Vörösmarty C J, Douglas E M, Green P A and Revenga C 2005 Geospatial indicators of emerging water stress: an application to Africa *AMBIO* **34** 230–6
Vörösmarty C J, Green P, Salisbury J and Lammers R B 2000 Global water resources: vulnerability from climate change and population growth *Science* **289** 284–8
Walvoord M A and Kurylyk B L 2016 Hydrologic impacts of thawing permafrost—a review *Vadose Zone J.* **15** 1–20
Wang P *et al* 2021 Potential role of permafrost thaw on increasing Siberian river discharge *Environ. Res. Lett.* **16** 034046
Warneke C *et al* 2009 Biomass burning in Siberia and Kazakhstan as an important source for haze over the Alaskan Arctic in April *Earth Syst. Sci. Lett.* **36** L02813
Wollheim W M, Peterson B J, Thomas S M, Hopkinson C H and Vorosmarty C J 2008 Dynamics of N removal over annual time periods in a suburban river network *J. Geophys. Res. Biogeosci.* **113** G03038
Wollheim W M, Stewart R J, Aiken G R, Butler K D, Morse N B and Salisbury J 2015 Removal of terrestrial DOC in aquatic ecosystems of a temperate river network *Geophys. Res. Lett.* **42** 6671–9
Woodhouse C A, Gray S T and Meko D M 2006 Updated streamflow reconstructions for the Upper Colorado River Basin *Water Resour. Res.* **42** W05415
WSAG 2016 The WBM model family (available at: http://wsag.unh.edu/wbm.html)
Wu P, Wood R and Stott P 2005 Human influence on increasing Arctic river discharges *Geophys. Res. Lett.* **32** L02703
Yang D, Marsh P and Ge S 2014 Heat flux calculations for Mackenzie and Yukon Rivers *Polar Sci.* **8** 232–41
Yang D, Robinson D, Zhao Y, Estilow T and Ye B 2003 Streamflow response to seasonal snow cover extent changes in large Siberian watersheds *J. Geophys. Res.* **108** 4578
Yang D, Ye D and Kane D L 2004 Streamflow changes over Siberian Yenisei River Basin *J. Hydrol.* **296** 59–80
Yang D, Zhao Y, Armstrong R, Robinson D and Brodzik M-J 2007 Streamflow response to seasonal snow cover mass changes over large Siberian watersheds *Geophys. Res. Lett.* **112** F02S22
Ye H, Cho H and Gustafson P E 1998 The changes in Russian winter snow accumulation during 1936–83 and its spatial patterns *J. Clim.* **11** 856–63
Zhang T *et al* 2005 Spatial and temporal variability in active layer thickness over the Russian Arctic drainage basin *J. Geophys. Res.* **110** D16101
Zhang T, Barry R G, Knowles K, Heginbottom J A and Brown J 2008 Statistics and characteristics of permafrost and ground-ice distribution in the Northern Hemisphere *Polar Geogr.* **31** 47–68
Zhang X J, Tang Q, Liu X, Leng G and Di C 2018 Nonlinearity of runoff response to global mean temperature change over major global river basin *Geophys. Res. Lett.* **45** 6109–16